

SHEAR WIND STRENGTH REQUIRED FOR DYNAMIC SOARING AT RIDGES

By G. Sachs and M. Mayrhofer

Submitted to SSA

ABSTRACT

Dynamic soaring is a flight method for extracting energy from horizontal wind the strength of which varies with altitude and which is termed shear wind. Behind ridges, significant shear wind conditions can exist so that dynamic soaring is possible. An optimal control technique is used for determining dynamic soaring trajectories at ridges for maximizing the energy transfer from the moving air to the sailplane. Particular emphasis is placed on achieving results for the required shear wind strength.

INTRODUCTION

Dynamic soaring is a flight method with the use of which a sailplane extracts energy from horizontally moving air. This method differs from well-known soaring techniques like thermaling and hang gliding where upwards moving air is used for feeding energy to the sailplane. For continuous dynamic soaring, it is necessary that the horizontally moving air is not constant but changes with altitude. This type of wind is called shear wind or shear flow.

The possibility of utilizing shear wind for soaring flight has been considered for quite a time, Refs. 1-15. Investigations based on energy estimates and numerical simulations provided valuable information about the wind strength necessary for dynamic soaring. Further, modern optimization techniques have been applied to the dynamic soaring problem, Refs. 16-19. Thus, precise results have been obtained for the minimum shear wind strength required for dynamic soaring and for the increase of the energy state of a sailplane when stronger shear wind conditions exist.

In mountainous regions, shear winds are possible at ridges. A wind coming over the top of a ridge produces a shear wind condition behind the ridge where a separation boundary between the wind area and a zone of still air exists. Such shear winds are used by model gliders for dynamic soaring, Ref. 20.

It is the purpose of this paper to determine optimal dynamic soaring trajectories at ridges for full-size sailplanes, with the goal of maximizing the energy transfer from the moving air to the vehicle. Related performance and control issues are considered. In particular, it will be shown which shear wind strength is required for dynamic soaring.

BASIC CONSIDERATIONS

Basically, an optimal dynamic soaring trajectory for maximum energy extraction from the moving air has a form as shown in Figure 1. Starting from point 1, the sailplane per-

forms a turn and then a climb against the wind. In the upper part of the trajectory, it turns into the wind and descends until it reaches a similar altitude level as before where it again starts a dynamic soaring maneuver like the one described. There may be a shear wind condition such that there is the same energy state of the sailplane at point 2 as compared with point 1 (same values for altitude and for inertial speed, respectively). This case represents an energy-neutral trajectory, meaning that dynamic soaring can be performed continuously without increasing or decreasing the energy state of the aircraft when reaching the end of a cycle as denoted by point 2. For treating energy-neutral dynamic soaring, it is sufficient to consider a single cycle as defined by the section between points 1 and 2 in Figure 1. A cycle which may be considered a basic element of an optimal dynamic soaring trajectory shows periodic properties as regards speed and altitude when comparing the final conditions at point 2 with the initial conditions at point 1.

The described form of optimal dynamic soaring trajectories may be classified as a bend type path. As an alternative, there can be spiral type trajectories, Figure 2. It can be shown (Ref. 16) that they are inferior to the bend type trajectories or equal at best with regard to the energy extraction from the moving air. The present paper will focus on the spiral type trajectories. This is because they may best fit to the limited spatial extent of the shear wind region at ridges in the lateral direction. Further, the spiral type trajectories are considered to be of a closed form, i.e., the beginning (point 1) and end (point 2) of a cycle coincide. This special spiral form may be termed an oval type trajectory. The oval characteristic is again considered to be adequate for the limited spatial shear wind extent.

The shear wind condition at a ridge is schematically illustrated in Figure 3. The wind is coming toward the hill from the left, with the angles of the arrows indicating the

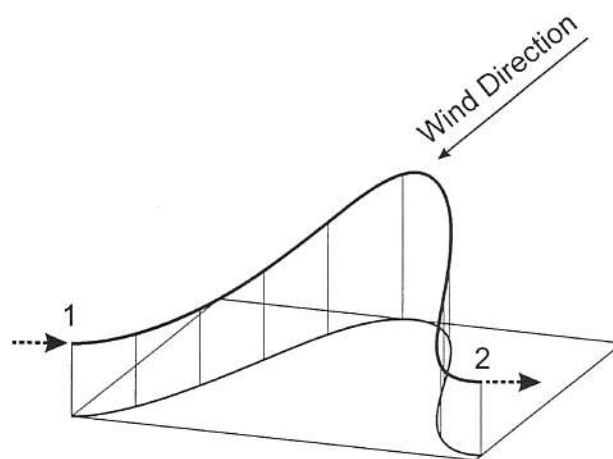
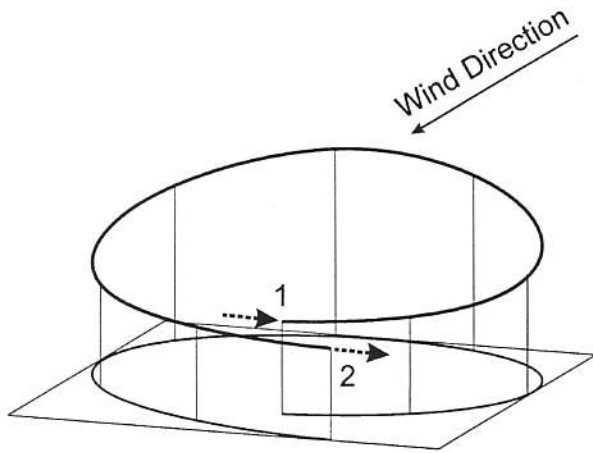


Fig. 1 Optimal dynamic soaring trajectory of bend type



direction of the wind. There is a boundary layer between the ridge surface and the free flow. The steep drop of the slope hill causes the wind together with the boundary layer to separate from the hill, resulting in a wind shear zone between areas of wind and of still air. This wind shear zone offers the possibility for dynamic soaring.

The thickness of the boundary layer increases and the shear wind gradient decreases with the distance from the ridge. Accordingly, dynamic soaring is most efficiently possible in a region close to the ridge. It is assumed that the shear wind characteristics do not change much for small distances from the ridge, in a region where dynamic soaring can be performed. The shear wind characteristics in a boundary layer, as illustrated in Figure 4 may be modeled as (Ref. 21)

$$V_w = V_{w,ref} \left(\frac{h - h_0}{h_{ref}} \right)^m \quad (1)$$

Fig. 2 Optimal dynamic soaring trajectory of spiral type

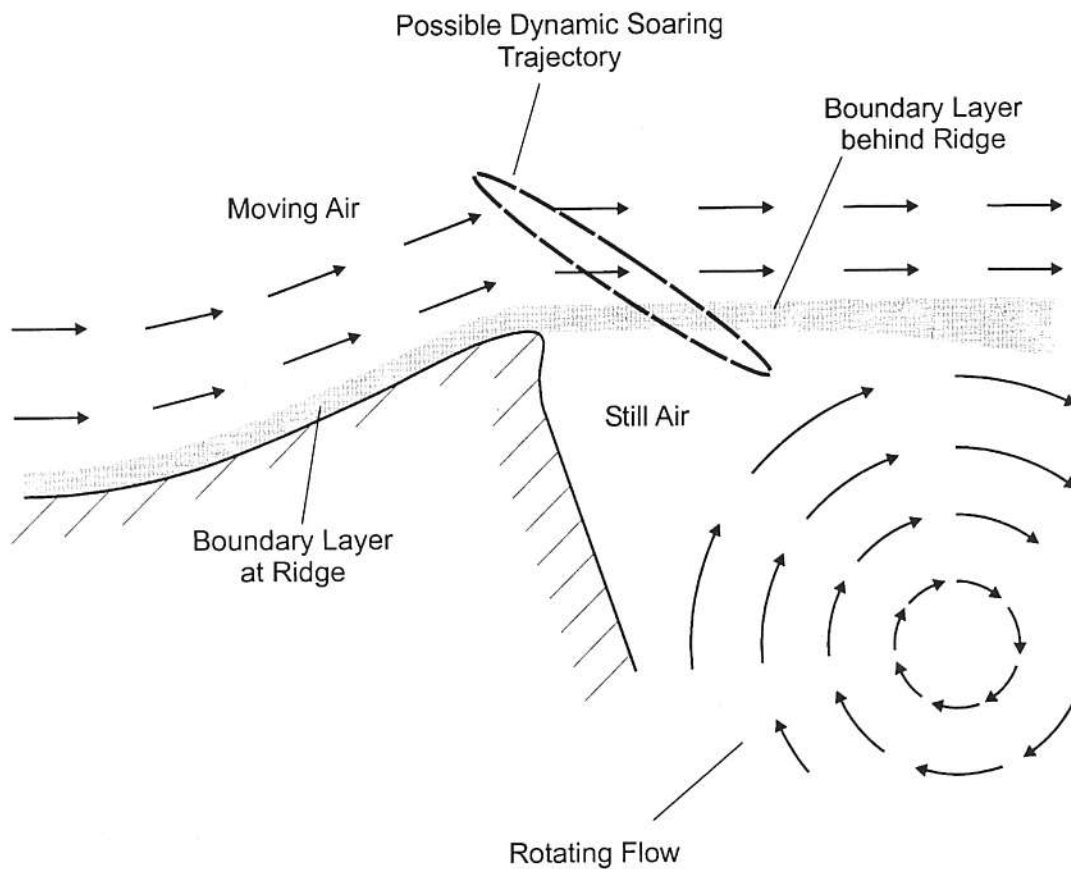


Fig. 3 Shear wind condition at ridge

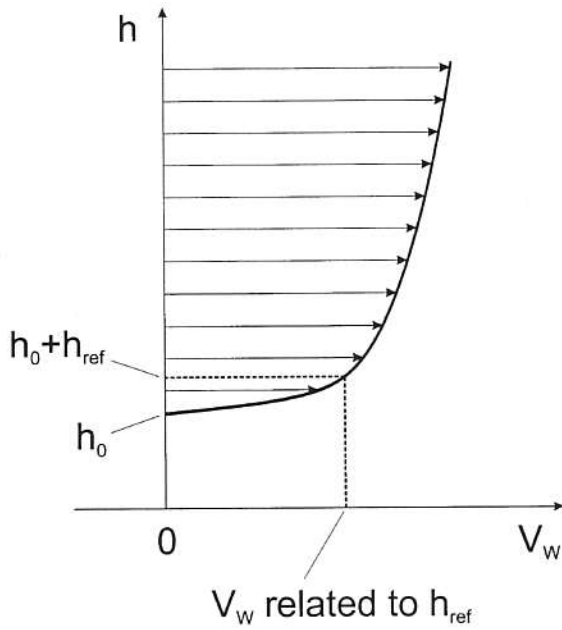


Fig. 4 Shear wind model

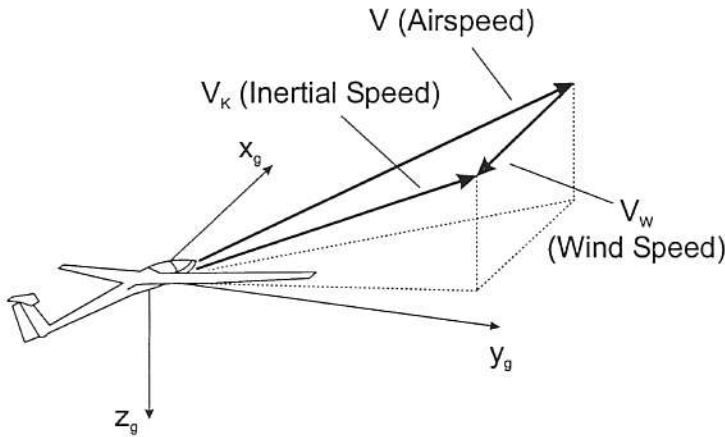


Fig. 5 Geodetic coordinate system and speed vectors for flight in horizontal shear wind

The quantities $V_{w,ref}$ and h_{ref} denote reference values which can be used for indicating the strength of the wind shear. This means that $V_{w,ref}$ provides a measure for the shear wind strength, evaluated at an altitude of $h = h_0 + h_{ref}$. In this paper, a reference value of $h_{ref} = 10\text{m}$ is applied. The exponent m in Eq. (1) relates to terrain surface properties which exert an effect on the shear wind characteristics. For a terrain surface with trees and woods the exponent can be set to $m = 0.2$ (Ref. 21).

The optimal control problem can now be formulated as to determine the minimum shear wind strength required for an energy-neutral trajectory. Accordingly, the following performance criterion may be introduced, using the reference value $V_{w,ref}$ as a measure for the shear wind strength:

$$J = V_{w,ref} \quad (2)$$

It is then necessary to determine the minimum of J for a cycle as described above, with the cycle time t_{cyc} introduced as the time interval between points 1 and 2 according to Figure 2.

Vehicle Dynamics and Optimal Control Problem Formulation

Sailplane dynamics are described using a point mass model with reference to an earth fixed coordinate system. The moving air is appropriately accounted for. Figure 5 shows the earth fixed reference system, with the x_g axis selected parallel to the wind, and the speed vectors describing the moving air and the motion of the sailplane. The equations of motion may be written as:

$$\begin{aligned} \dot{u}_{Kg} &= -a_{u1} \frac{D}{m} + a_{u2} \frac{L}{m} \\ \dot{v}_{Kg} &= -a_{v1} \frac{D}{m} + a_{v2} \frac{L}{m} \\ \dot{w}_{Kg} &= -a_{w1} \frac{D}{m} + a_{w2} \frac{L}{m} - g \\ \dot{x}_g &= u_{Kg} \\ \dot{y}_g &= v_{Kg} \\ \dot{h} &= -w_{Kg} \end{aligned} \quad (3)$$

where

$$\begin{aligned} a_{u1} &= \cos \gamma_a \cos \chi_a, & a_{u2} &= \cos \mu_a \sin \gamma_a \cos \chi_a + \sin \mu_a \sin \chi_a \\ a_{v1} &= \cos \gamma_a \sin \chi_a, & a_{v2} &= \cos \mu_a \sin \gamma_a \sin \chi_a - \sin \mu_a \cos \chi_a \\ a_{w1} &= -\sin \gamma_a, & a_{w2} &= \cos \mu_a \cos \gamma_a \end{aligned} \quad (4)$$

The aerodynamic forces are drag and lift which read:

$$\begin{aligned} L &= C_L(\rho/2)V^2S \\ D &= C_D(\rho/2)V^2S \end{aligned} \quad (5)$$

Drag characteristics can be modeled as:

$$C_D = C_{D0} + KC_L^2 \quad (6)$$

where the lift coefficient C_L is a control which is determined by optimality computations.

The aerodynamic forces are dependent on the airspeed vector \mathbf{V} , while the motion of the sailplane with regard to the earth is described by the inertial speed vector $\mathbf{V}_K = (u_{kg}, v_{kg}, w_{kg})^T$. They are related to each other by the following expression (Figure 5):

$$\mathbf{V} = \mathbf{V}_k - \mathbf{V}_w \quad (7a)$$

With the use of $\mathbf{V}_w = (V_w, 0, 0)^T$, Eq. (7) may be rewritten as

$$\mathbf{V} = (u_{kg} + V_w, v_{kg}, w_{kg})^T \quad (7b)$$

where

$$V = \sqrt{(u_{kg} + V_w)^2 + v_{kg}^2 + w_{kg}^2} \quad (7c)$$

Two of the angles of the aerodynamic coordinate system used in Eqs. (3) and (4) are determined by:

$$\begin{aligned} \sin \gamma_a &= -\frac{w_{kg}}{V} \\ \tan \chi_a &= \frac{v_{kg}}{u_{kg} + V_w} \end{aligned} \quad (8)$$

The remaining angle, μ_a , which describes banking of the lift vector is a control. It is determined by optimality computations.

For oval type cycle of an energy-neutral trajectory, the following boundary conditions hold:

$$\begin{aligned} u_{kg}(0) &= u_{kg}(t_{cyc}), v_{kg}(0) = v_{kg}(t_{cyc}), w_{kg}(0) = w_{kg}(t_{cyc}), \\ h(0) &= h(t_{cyc}), x_g(0) = x_g(t_{cyc}) = 0, y_g(0) = y_g(t_{cyc}) = 0 \end{aligned} \quad (9)$$

For w_{kg} , the boundary condition can be chosen as $w_{kg} = 0$ since there is a point of the trajectory where this value holds. This implies that beginning and end of a cycle (points 1 and 2 in Figure 2) are correspondingly selected, yielding

the smallest h values with $h(0) = h(t_{cyc})$.

The controls are subject to the following inequality constraints:

$$\begin{aligned} C_{Lmin} &\leq C_L \leq C_{Lmax} \\ -90\text{deg} &< \mu_a \leq 90\text{deg} \end{aligned} \quad (10)$$

The optimal control problem can now be formulated as to determine the controls, the initial conditions $V_k(0) = (u_{kg}(0), v_{kg}(0), w_{kg}(0))^T$ and $H(0)$ and the optimal cycle time t_{cyc} which minimize the performance criterion $J = V_{w,ref}$ subject to the dynamic system Eq. (3), the boundary conditions Eq. (9) and the controls inequality constraints Eq. (10):

$$\bar{u}(t) = (C_A(t), \mu_a(t))^T \quad (11)$$

is approximated by a parameter vector p . With reference to a subdivision of the time period:

$$0 = t_1 < t_1 < \dots < t_{m-1} < t_m = t_{cyc} \quad (12)$$

the following relation is applied:

$$\bar{u}(t) = U_j(p, t), t_j \leq t \leq t_{j+1} \quad (13)$$

The function U_j is an estimation of the control for interval j , with $j=1, \dots, m-1$.

The controls were determined using linear functions. For given initial conditions, the equations of motion, Eq. (3) can be integrated using the estimated control values. Thus, an evaluation with regard to the performance criterion and the boundary conditions is possible. This results in a non-linear problem where the performance criterion:

$$J = V_{w,ref}(\bar{p}) \quad (14)$$

is to be minimized and the boundary conditions have to be met:

$$b(\bar{p}, t_{cyc}) = 0 \quad (15)$$

For solving the described optimal control problem, efficient numerical optimization methods and computational techniques are required which are capable of coping with complex functional relationships including various kinds of constraints. The numerical investigation was performed using the parameterization optimization technique ALTOS of Ref. 22 with the graphical environment GESOP of Ref. 23.

Results for Optimal Energy-Neutral Trajectories

Results for an optimized oval energy-neutral trajectory of dynamic soaring at a ridge are shown in Figures 6-9 for a sailplane with a maximum lift-to-drag ratio of $(L/D)_{max} = 45$ and a wing loading of $m/S = 50\text{kg/m}^2$, applying

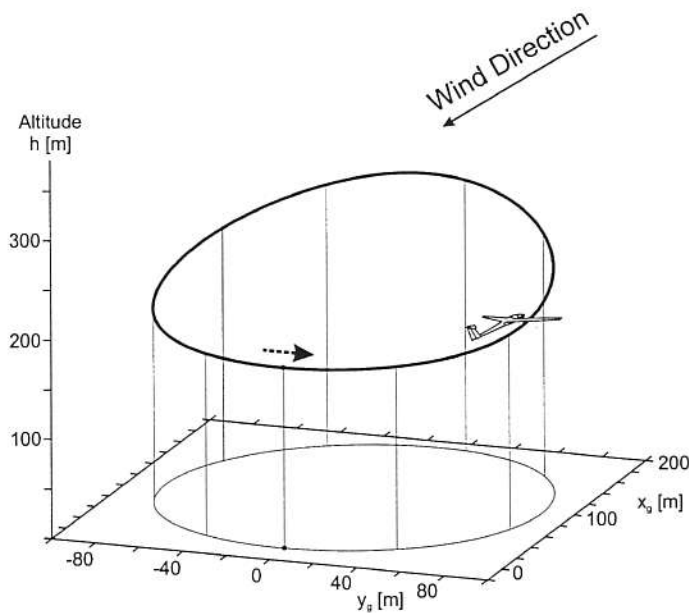


Fig. 6 Optimal oval-type dynamic soaring trajectory for sailplane with $(L/D)_{max} = 45$ and $m/S = 50 \text{ kg/m}^2$ (h referenced to bottom of ridge)

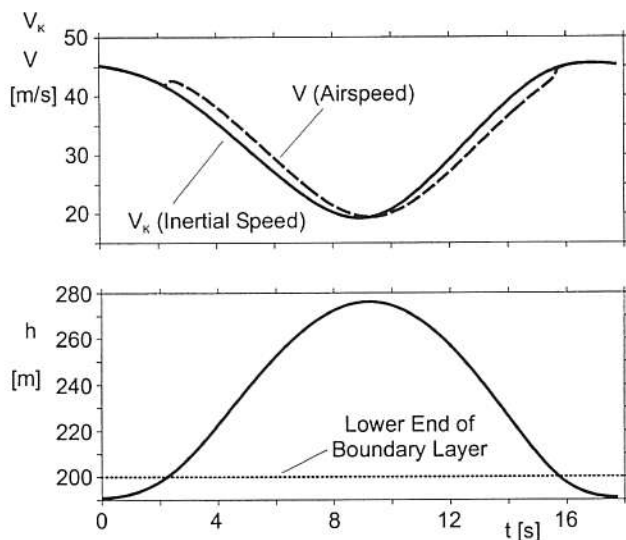


Fig. 7 Speeds and altitude of oval-type dynamic soaring trajectory for sailplane with $(L/D)_{max} = 45$ and $m/S = 50 \text{ kg/m}^2$ (h referenced to bottom of ridge)

quadratic drag polar characteristics according to Eq. (6). The altitude of the ridge is assumed to be 200 m. From the optimization computations it follows as a main result that a shear wind strength of $V_{w,ref} = 2.44 \text{ m/s}$ at $h_{ref} = 10\text{m}$ is required for continuously performing dynamic soaring. The cycle time amounts to $t_{cyc} = 17.76 \text{ s}$. Figure 6 provides a perspective view on the trajectory, showing the motion in the three coordinates.

Figure 7 presents the history of state variables providing more quantitative information of the motion. Airspeed is larger than inertial speed during the first part of a cycle because the sailplane moves in a direction against the wind. The opposite holds for the second part. As an important result for the practical utilization of the optimal dynamic soaring trajectory, the maximum of the airspeed stays well below possible limits for sailplanes which are in the order of 90 m/s.

The altitude time history is also presented in Figure 7 showing that the altitude range of the optimal dynamic soaring cycle is about 85 m. The upper turn from a direction against the wind into the wind is performed at an altitude where the wind speed is comparatively high. This characteristic of the upper turn which is most important for the energy transfer from the moving air to the sailplane indicates that the wind speed is fully utilized for achieving an energy gain.

In figure 8, the behavior of the optimal controls is illustrated. The lifting capability of the sailplane is used to a large extent. This particularly holds for the turn into the wind at the upper part of the trajectory where the lift coef-

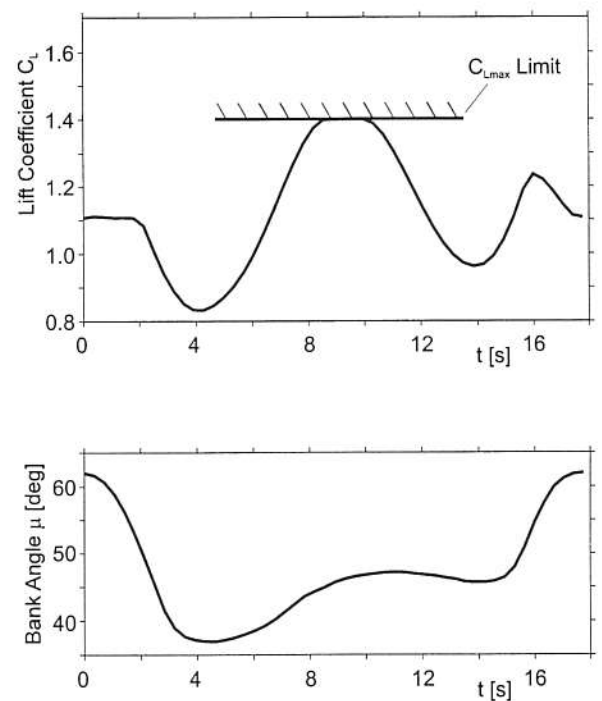


Fig. 8 Lift coefficient and bank angle of oval-type dynamic soaring trajectory for sailplane with $(L/D)_{max} = 45$ and $m/S = 50 \text{ kg/m}^2$

efficient C_L takes on large values. Here, even the maximum lift coefficient constraint, C_{Lmax} , becomes active. For the turn into a direction against the wind at the lower part of the trajectory, the lift coefficient is reduced. It may be of interest to compare the behavior of the lift coefficient and the airspeed which are, to a certain degree, complementary to each other in order to produce the optimal lift behavior. Bank angle control μ which is also illustrated in Figure 8 is applied without reaching its limits. It takes on its largest values during the turn against the wind, in the lower part of the trajectory.

An important issue concerns the load on pilot and vehicle, which can be described by the load factor. This is illustrated in Figure 9 which presents the load factor time history. It shows that the load factor does not reach extreme values. Most significant for the practical utilization, the load

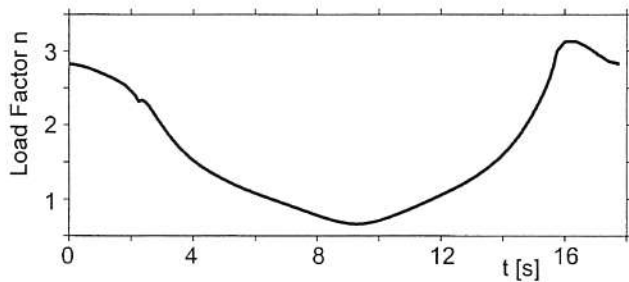


Fig. 9 Load factor of oval-type dynamic soaring trajectory for sailplane with $(L/D)_{max} = 45$ and $m/S = 50 \text{ kg/m}^2$

factor maximum stays well below acceptable limits which are in the order of $n=4.5$.

An evaluation of systematic optimization computations is presented in Figure 10 which shows the minimum shear wind required for optimum energy-neutral trajectories in relation to the maximum lift-drag ratio of sailplanes, applying quadratic drag polar characteristics according to Eq. (6) and a wing loading of $m/S=50\text{kg/m}^2$. The presented data cover a wide range of maximum lift-to-drag ratios of sailplanes. As a main result, the required shear wind strength $V_{w,ref}$ is at a moderate level which can be considered as realistic and which is often exceeded in existing shear wind situations at ridges. This result holds for the entire range of maximum lift-to-drag ratios, including sailplanes of lower aerodynamic performance.

In Figure 10, the results for existing sailplanes are also presented. The models for their aerodynamic characteristics are more complex when compared with the quadratic drag polar applied in Eq. (6). They account for higher order terms and for non-symmetrical drag characteristics. The results

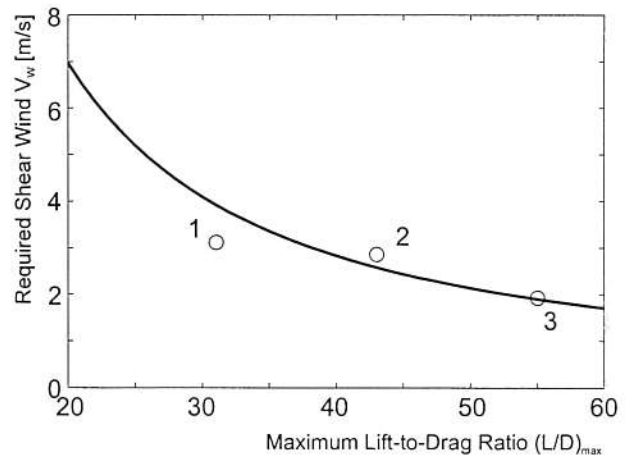


Fig. 10 Required shear wind strength V_w related to h_{ref} for optimal dynamic soaring (oval type trajectory, $m/S = 50 \text{ kg/m}^2$)

Sailplane 1 similar to Ka 6E ($m/S = 23.0 \text{ kg/m}^2$), Club Class
Sailplane 2 similar to LS 7 ($m/S = 49.7 \text{ kg/m}^2$), Standard Class
Sailplane 3 similar to ASW 22 ($m/S = 46 \text{ kg/m}^2$), Open Class

presented in Figure 10 show that the values for these sailplanes which may be regarded as representative for different sailplane classes are in agreement with the result obtained for the quadratic drag polar modeling.

CONCLUSIONS

Dynamic soaring which is a flight method for extracting energy from horizontally moving air is considered for wind regions behind ridges where significant shear flow conditions can exist.

An optimal control technique is used for determining energy-neutral dynamic soaring trajectories such that dynamic soaring is continuously possible. An evaluation is presented for the required shear wind strength depending on the maximum lift-to-drag ratio of sailplanes. As a main result, the required shear wind strength is at a level which can be considered as existent in realistic shear wind situations. Furthermore, the maximum values of airspeed and load factor of dynamic soaring trajectories stay well below limits acceptable for sailplanes.

REFERENCES

- 1 Prandtl, L., Beobachtungen über den dynamischen Segelflug, Zeitschrift für Flugtechnik and Motorluftschiffahrt, 21. Jahrg., S. 116, 1930.
- 2 Idrac, P., Experimentelle Untersuchungen über den

Segelflug, Oldenbourg-Verlag, Berlin, 1932.

3 Klemperer, W., A Review on the Theory of Dynamic Soaring, OSTI-Bericht S. 498-501, 1958.

4 Contensou, P., Optimization du Vol Plane dans un Vent Horizontal Variable, Congress of Appl. Mechanics, Stanford University, 1968.

5 Fritsch, E., Zum dynamischen Segelflug, Aero-Revue, Heft 12, S. 669-672, 1971, Heft 1, S. 40, 1972.

6 Hendriks, F., Dynamic Soaring, Dissertation, University of California, Los Angeles, 1972.

7 Hendriks, F., Dynamic Soaring in Shear Flow, AIAA Paper 74-1003, 1974.

8 Tromsdorff, W., Flugmechanische und technische Voraussetzungen für den Dynamischen Segelflug mit bemanntem Fluggerät, OSTIV-Bericht, 1974.

9 Trommsdorff, W., Voraussetzungen für die Durchführung des dynamischen Segelflugs, Aerokurier, Heft 12, S. 1106-1107, 1976.

10 Renner, I., Dynamischer Segelflug, Aerokurier, Heft 12, S. 1104-1105, 1976.

11 Gorisch, W., Energy Exchange between a Sailplane and Moving Air Masses Under Instationary Flight Conditions with Respect to Dolphin Flight and Dynamic Soaring, Aero-Revue, Heft 11, S. 691-692 (Teil 1), Heft 12, S. 751-752 (Teil 2), 1976, Erratum, Heft 3, S. 182, 1977.

12 Gorisch, W., Zum Problem des dynamischen Segelflugs in der horizontalen Grenzschicht zwischen ruhender und bewegter Luftmasse, Aerokurier, Heft 9 S. 855-858, 1977.

13 Nottebaum, T., Ein Rechenprogramm zur Simulation des Dynamischen Segelflug, DGLR-Jahrbuch, S. 329-338, 1987.

14 Goebel, O., Scherwindmessungen an Bord einer Piper PA 18 und Auslegung eines Modellsegelflugzeugs für den

Dynamischen Segelflug, DGLR-Jahrbuch, S. 332-328, 1987.

15 Nottebaum, T.; Goebel, O., Simulation optimaler Flugbahnen des dynamischen Segelflugs und Auslegung eines Modellflugzeugs, Zeitschrift für Flugwissenschaften und Weltraumforschung, Vol. 13, s. 48-56, 1989.

16 Sachs, G., Minimalbedingungen für den dynamischen Segelflug, Zeitschrift für Flugwissenschaften und Weltraumforschung, Vol. 13, pp-188-198, 1989.

17 Sachs, G.; Knoll, A.; Lesch, K., Optimal Control for Maximum Energy Extraction from Wind Shear, AIAA Guidance, Navigation and Control Conference, AIAA Paper 89-3490, 1989.

18 Sachs, G.; Knoll A.; Lesch, K., Optimal utilization of wind energy for dynamic soaring, Technical Soaring, Vol. 15, No. 2, pp. 48-55, 1991.

19 Sachs, G., Optimal Wind Energy Extraction for Dynamic Soaring - In: Applied Mathematics in Aerospace Science and Engineering, Plenum Press, New York and London, Vol. 44, pp. 221-237, 1994.

20 Fogel, L., Dynamic Soaring? S&E Modeler Magazine, Vol. 4-1, 1999.

21 Swolinski, M., Beiträge zur Modellierung von Scherwind für Gafahrdungsuntersuchungen. Dissertation, Fakultät für Maschinenbau und Elektrotechnik der Technischen Universität Carolo-Wilhelmina zu Braunschweig, 1986.

22 N.N., ALTOS - Software User Manual, Institut für Flugmechanik und Regelung, University of Stuttgart, August 1996.

23 N.N., GESOP (Graphical environment for simulation and Optimization), Softwaresystem für Bahnoptimierung, Institut für Robotik und Systemdynamik, DLR, Oberpfaffenhofen, 1993.